MONOCLONAL ANTIBODIES IN IMMUNODIAGNOSIS AND IMMUNOTHERAPY
Volume XX, Number XX, 2024

DOI: 10.1089/mab.2023.0016

Development of a Sensitive Anti-Mouse CD39 Monoclonal Antibody (C_{39}Mab-1) for Flow Cytometry and Western Blot Analyses

Yuki Okada, Hiroyuki Suzuki, Mika K. Kaneko, and Yukinari Kato

CD39 is involved in adenosine metabolism by converting extracellular ATP to adenosine. As extracellular adenosine plays a critical role in the immune suppression of the tumor microenvironment, the inhibition of CD39 activity by monoclonal antibodies (mAbs) is one of the important strategies for tumor therapy. This study developed specific and sensitive mAbs for mouse CD39 (mCD39) using the Cell-Based Immunization and Screening method. The established anti-mCD39 mAb, C_{39}Mab-1 (rat IgG_{2a}, kappa), reacted with mCD39-overexpressed Chinese hamster ovary-K1 (CHO/mCD39) by flow cytometry. The kinetic analysis using flow cytometry indicated that the dissociation constant of C_{39}Mab-1 for CHO/mCD39 was 7.3×10^{-9} M. Furthermore, C_{39}Mab-1 detected the lysate of CHO/mCD39 by western blot analysis. These results indicated that C_{39}Mab-1 is useful for the detection of mCD39 in many functional studies.

Keywords: mouse CD39, monoclonal antibody, the Cell-Based Immunization and Screening, CBIS

Introduction

Extracellular adenosine, generated by the hydrolysis of extracellular ATP (eATP), mediates an immunosuppressive tumor microenvironment (TME).[1] The high concentration of eATP can be found in solid tumors due to the passive release of cell death and active secretion by tumor cells and other subsets in the TME.[2] Following the release of eATP, CD39 (ectonucleoside triphosphate diphosphohydrolase 1; encoded by *ENTPD1*) hydrolyzes eATP to ADP and AMP. Then, another rate-limiting ectoenzyme, CD73 (5′-nucleotidase; encoded by NT5E), dephosphorylates AMP into adenosine.[3]

Growing body of evidence suggests that adenosine-mediated immunosuppression is critical for tumor immune evasion. Various tumors showed the elevated expression of CD39, which promotes the local accumulation of adenosine surrounding tumors.[4] The adenosine-mediated immunosuppressive effect functions via four G protein-coupled type 1 purinergic (P1) receptors, A_1, A_{2A}, A_{2B}, and A_3 expressed on immune cells.[5] Among the four P1 receptors, the A_{2A} and A_{2B} are G_S-coupled receptors and trigger intracellular cAMP accumulation. The cAMP signaling mediates immunosuppression by activation of effectors, including protein kinase A.[6]

Sitkovsky's group first reported the immunosuppressive effects of the A_{2A} receptor *in vivo*.[7] Inflammatory stimuli that caused minimal tissue damage in wild-type mice were sufficient to induce extensive tissue damage, more prolonged and higher levels of proinflammatory cytokines, and individual death in mice lacking the A_{2A} receptor.[7] The group also showed genetic evidence of the importance of the A_{2A} receptor in tumor immunity.[8] These findings impacted antitumor immunity by CD39–adenosine–A_2 receptor axis and several landmark studies have developed multiple strategies targeting adenosine metabolism.[3,9]

The development of anti-CD39 monoclonal antibodies (mAbs) is a strategy to modulate the adenosine metabolism. A preclinical study revealed that an anti-mouse CD39 (mCD39) mAb (clone B66), which can inhibit mCD39 activity *in vitro*, exhibited the antitumor effect in syngeneic models by the monotherapy and combination therapy with the programmed cell death-1 (PD-1) blockade.[10] This study also showed that B66 triggers an eATP–P2X7–inflammasome–IL-18 pathway that promotes tumor immunity and overcomes anti-PD-1 resistance.[10] The anti-human

Department of Antibody Drug Development, Tohoku University Graduate School of Medicine, Sendai Japan.

CD39 mAbs (clones TTX-030, IPH5201, and SRF-617) were designed to inhibit CD39 enzymatic activity via allosteric inhibition and minimize Fc receptor-mediated engagement to avoid the side effects.[10,11] These mAbs have entered the clinical trials for solid tumors with a combination of chemotherapeutic agents or immune checkpoint inhibitors.[3]

Using the Cell-Based Immunization and Screening (CBIS) method, we have developed many mAbs against membrane proteins, such as CD19,[12] CD20,[13,14] CD133,[15] EpCAM,[16,17] HER2,[18] HER3,[19] KLRG1,[20] TIGIT,[21] TROP2,[22,23] programmed cell death ligand 1 (PD-L1),[24] podoplanin,[25–36] and CD44.[37,38] The CBIS method includes the immunization of antigen-overexpressed cells and high-throughput hybridoma screening using flow cytometry. Anti-chemokine receptors mAbs, including anti-mouse CCR3,[39] anti-mouse CCR8,[40] and anti-human CCR9[41] mAbs, were also successfully developed using the CBIS method.

In this study, novel anti-mCD39 mAbs were developed by the CBIS method. We further evaluated its applications, including flow cytometry and western blot analyses.

Materials and Methods

Preparation of cell lines

LN229, Chinese hamster ovary (CHO)-K1, and P3X63Ag8U.1 (P3U1) were obtained from the American Type Culture Collection (Manassas, VA).

The synthesized DNA (Eurofins Genomics KK) encoding mCD39 (Accession No.: NM_009848) was subsequently subcloned into a pCAGzeo_nPA-cRAPMAP vector, which is derived from a pCAGzeo vector (FUJIFILM Wako Pure Chemical Corporation, Osaka, Japan), *N*-terminal PA tag,[42–44] and *C*-terminal RAP tag[45,46] + MAP tag.[47,48] The amino acid sequences of the tag system were as follows: PA tag, 12 amino acids (GVAMPGAEDDVV); RAP tag, 12 amino acids (DMVNPGLEDRIE); and MAP tag, 12 amino acids (GDGMVPPGIEDK). The PA tag can be detected by an anti-human podoplanin mAb (clone NZ-1).[42–44,49–61] The mCD39 plasmid was transfected into CHO-K1 and LN229 cells, using a Neon transfection system (Thermo Fisher Scientific Inc., Waltham, MA). Stable transfectants were established through cell sorting using a cell sorter (SH800; Sony Corp., Tokyo, Japan), after which cultivation in a medium, containing 0.5 mg/mL of Zeocin (InvivoGen, San Diego, CA) was conducted.

CHO-K1, mCD39-overexpressed CHO-K1 (CHO/mCD39), and P3U1 were cultured in a Roswell Park Memorial Institute (RPMI)-1640 medium (Nacalai Tesque, Inc., Kyoto, Japan), with 10% heat-inactivated fetal bovine serum (FBS; Thermo Fisher Scientific Inc.), 100 units/mL of penicillin, 100 μg/mL of streptomycin, and 0.25 μg/mL of amphotericin B (Nacalai Tesque, Inc.). LN229 and mCD39-overexpressed LN229 (LN229/mCD39) were cultured in Dulbecco's Modified Eagle Medium (DMEM; Nacalai Tesque, Inc.), supplemented with 10% FBS, 100 U/mL of penicillin, 100 μg/mL streptomycin, and 0.25 μg/mL amphotericin B.

All cells were grown in a humidified incubator at 37°C, at an atmosphere of 5% carbon dioxide and 95% air.

Antibodies

An anti-mCD39 mAb (clone 5F2, mouse IgG_1, kappa) was purchased from BioLegend (San Diego, CA). Alexa Fluor 488-conjugated anti-rat IgG and Alexa Fluor 488-conjugated anti-mouse IgG secondary Abs were purchased from Cell Signaling Technology, Inc. (Danvers, MA).

Production of hybridomas

A 5-week-old Sprague–Dawley rat was purchased from CLEA Japan (Tokyo, Japan). The animal was housed under specific pathogen-free conditions. All animal experiments were performed according to the relevant guidelines and regulations to minimize animal suffering and distress in the laboratory. The Animal Care and Use Committee of Tohoku University (Permit No.: 2019NiA-001) approved animal experiments. The rat was monitored daily for health during the complete 4-week duration of the experiment. A reduction of more than 25% of the total body weight was defined as a humane endpoint. During the sacrifice, the rat was euthanized through cervical dislocation, after which death was verified through respiratory and cardiac arrest.

To develop mAbs against mCD39, we intraperitoneally immunized one rat with LN229/mCD39 (1×10^9 cells) plus Imject Alum (Thermo Fisher Scientific Inc.). The procedure included three additional injections every week (1×10^9 cells/rat), which were followed by a final booster intraperitoneal injection (1×10^9 cells/rat), 2 days before harvesting spleen cells. The harvested spleen cells were subsequently fused with P3U1 cells, using PEG1500 (Roche Diagnostics, Indianapolis, IN), after which hybridomas were grown in the RPMI-1640 medium with 10% FBS, 100 units/mL of penicillin, 100 μg/mL of streptomycin, and 0.25 μg/mL of amphotericin B. For the hybridoma selection, hypoxanthine, aminopterin, and thymidine (Thermo Fisher Scientific Inc.) were added into the medium. The supernatants were subsequently screened using flow cytometry using CHO/mCD39 and CHO-K1.

Purification of mAbs

The cultured supernatants of C_{39}Mab-1-producing hybridomas were collected through centrifugation at 2330 *g* for 5 minutes, followed by filtration using Steritop (0.22 μm, Merck KGaA, Darmstadt, Germany). The filtered supernatants were subsequently applied to 1 mL of Protein G Sepharose 4 Fast Flow (GE Healthcare, Chicago, IL). After washing with phosphate-buffered saline (PBS), bound antibodies were eluted with an IgG elution buffer (Thermo Fisher Scientific Inc.), followed by immediate neutralization of eluates, using 1 M Tris-HCl (pH 8.0). Finally, the eluates were concentrated, after which the elution buffer was replaced with PBS using Amicon Ultra (Merck KGaA).

Flow cytometric analysis

CHO-K1 and CHO/mCD39 were harvested after a brief exposure to 0.25% trypsin and 1 mM ethylenediaminetetraacetic acid (Nacalai Tesque, Inc.). The cells were subsequently washed with 0.1% bovine serum albumin in PBS and treated with 0.001, 0.01, 0.1, and 1 μg/mL of primary mAbs for 30 minutes at 4°C. The cells were treated with Alexa Fluor 488-conjugated anti-rat IgG or Alexa Fluor 488-conjugated anti-mouse IgG (1:2,000). The fluorescence data were collected using the SA3800 Cell Analyzer (Sony Corp.).

Determination of dissociation constant through flow cytometry

CHO/mCD39 were suspended in 100 μL serially diluted C_{39}Mab-1 for 30 min at 4°C. The cells were treated with 50 μL of Alexa Fluor 488-conjugated anti-rat IgG (1:200). The fluorescence data were collected, using the SA3800 Cell Analyzer. The dissociation constant (K_D) was subsequently calculated by fitting saturation binding curves to the built-in; one-site binding models in GraphPad PRISM 8 (GraphPad Software, Inc., La Jolla, CA).

Western blot analysis

Cell lysates were boiled in sodium dodecyl sulfate sample buffer (Nacalai Tesque, Inc.). The protein lysates (10 μg) were separated on 5%–20% polyacrylamide gels (FUJIFILM Wako Pure Chemical Corporation) and transferred onto polyvinylidene difluoride membranes (Merck KGaA). After blocking with 4% skim milk (Nacalai Tesque, Inc.) in PBS with 0.05% Tween 20, the membranes were incubated with 10 μg/mL of C_{39}Mab-1, 1 μg/mL of an anti-isocitrate dehydrogenase 1 (IDH1) mAb (clone RcMab-1),[62,63] or 1 μg/mL of NZ-1 (an anti-PA tag mAb). The membranes were then incubated with peroxidase-conjugated anti-rat immunoglobulins (diluted 1:10,000; Sigma-Aldrich Corp., St. Louis, MO). Finally, the protein bands were detected with ImmunoStar LD (FUJIFILM Wako Pure Chemical Corporation) using a Sayaca-Imager (DRC Co. Ltd., Tokyo, Japan).

Results

Development of anti-mCD39 mAbs by the CBIS method

To develop anti-mCD39 mAbs, one rat was immunized with LN229/mCD39 cells (Fig. 1A). The spleen was then excised from the rat, and splenocytes were fused with P3U1 cells (Fig. 1B). The developed hybridomas were subsequently seeded into ten 96-well plates and cultivated for 6 days. The positive wells were screened by the selection of mCD39-expressing cell-reactive and CHO-K1-nonreactive supernatants, using flow cytometry (Fig. 1C). After the limiting dilution and several additional screenings, an anti-mCD39 mAb, C_{39}Mab-1 (rat IgG_{2a}, kappa), was finally established (Fig. 1D).

Flow cytometric analyses

We conducted flow cytometry using anti-mCD39 mAbs (C_{39}Mab-1 and 5F2) against CHO/mCD39 and CHO-K1 cell lines. C_{39}Mab-1 recognized CHO/mCD39 cells dose-dependently at 1, 0.1, 0.01, and 0.001 μg/mL. In contrast, 5F2 needed more than 0.01 μg/mL for the detection of CHO/mCD39 (Fig. 2A). Parental CHO-K1 cells were not recognized even at 1 μg/mL of all mAbs (Fig. 2B).

Kinetic analyses of C_{39}Mab-1 against mCD39-overexpressed cells using flow cytometry

To determine the K_D of C_{39}Mab-1 with mCD39-overexpressed cells, we conducted kinetic analysis by flow cytometry using CHO/mCD39 (Fig. 3). The geometric mean of the fluorescence intensity was plotted versus the concentration of C_{39}Mab-1. The K_D value of C_{39}Mab-1 for CHO/mCD39 was determined as 7.3×10^{-9} M.

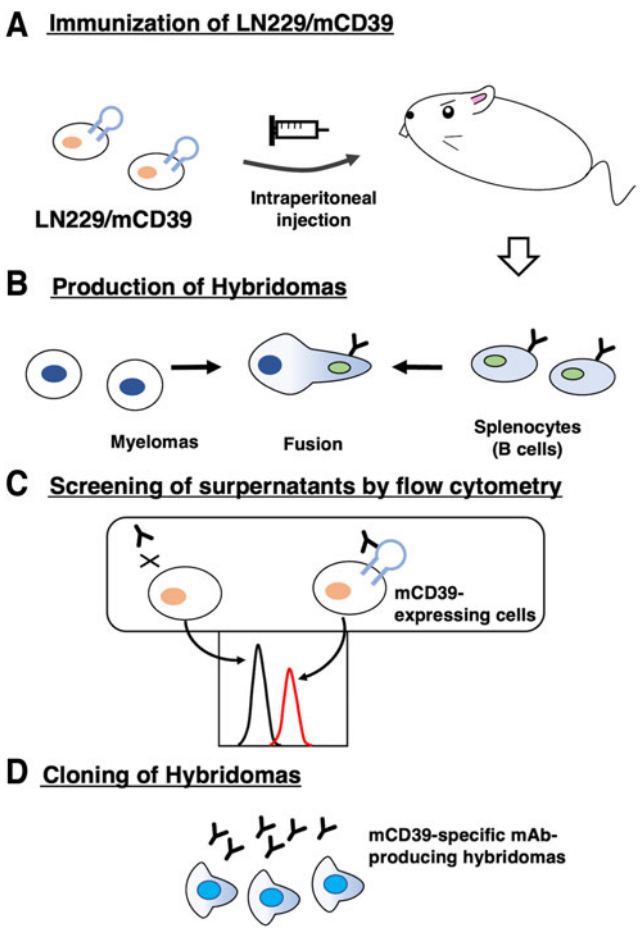

FIG. 1. A schematic illustration demonstrating the production of anti-mCD39 mAbs. **(A)** CD39 is anchored to the membrane by two transmembrane domains at the two ends of the molecule. LN229/mCD39 cells were immunized into a Sprague–Dawley rat, using an intraperitoneal injection. **(B)** The spleen cells were then fused with P3U1 cells. **(C)** Subsequently, the culture supernatants were screened through flow cytometry to select anti-mCD39 mAb-producing hybridomas. **(D)** After limiting dilution and some additional screenings, anti-mCD39 mAbs were finally established. mAbs, monoclonal antibodies.

Western blot analysis

Western blotting was performed to further assess the specificity of C_{39}Mab-1. The cell lysates of CHO-K1 and CHO/mCD39 were probed. As shown in Figure 4A, C_{39}Mab-1 detected mCD39 as a ~100-kDa band. An anti-PA tag mAb (clone NZ-1) recognized the lysates from CHO/mCD39 (~100 kDa, mainly) (Fig. 4B). These results indicated that C_{39}Mab-1 can detect mCD39 specifically by western blot analysis.

Discussion

In the TME, extracellular levels of ATP can reach 100–500 μM compared to the nanomolar order in normal tissues.[9] CD39 can rapidly hydrolyze and convert to adenosine in

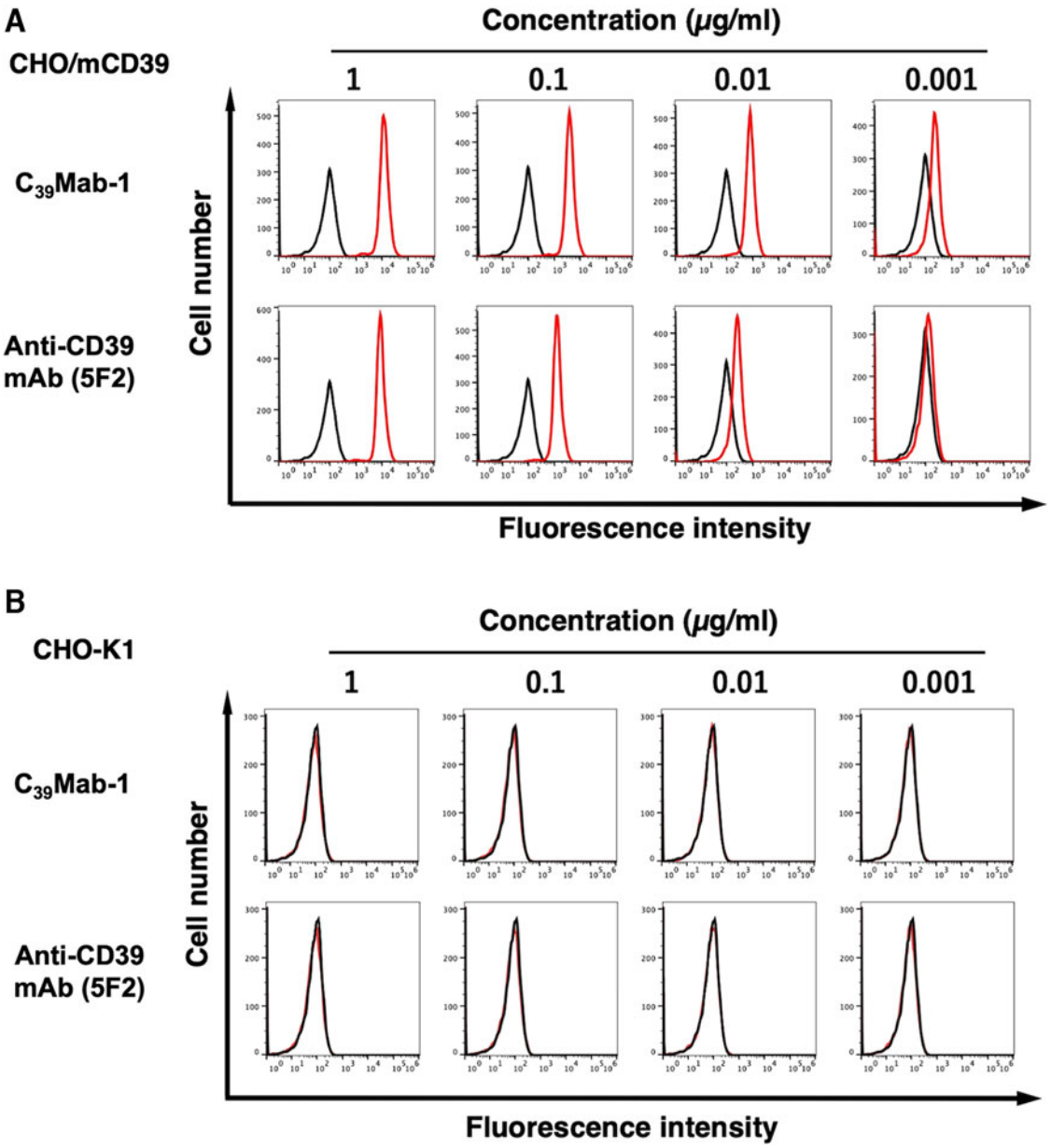

FIG. 2. Flow cytometry to mCD39-overexpressing cells using anti-mCD39 mAbs. CHO/mCD39 **(A)** and CHO-K1 **(B)** cells were treated with 0.001–1 μg/mL of C_{39}Mab-1 and 5F2, followed by treatment with Alexa Fluor 488-conjugated anti-rat IgG (for C_{39}Mab-1) or Alexa Fluor 488-conjugated anti-mouse IgG (for 5F2). The black line represents the negative control.

cooperation with CD73. In this TME, an enzymatic inhibitor of CD39 is the rational mechanism to inhibit the production of immunosuppressive adenosine. The clinically tested an anti-CD39 mAb, TTX-030 (human IgG_4), had a subnanomolar EC_{50} for human CD39-overexpressed CHO cells in the flow cytometry-based assay like in Figure 3. Furthermore, TTX-030 allosterically inhibited the enzymatic activity of CD39 in the recombinant human CD39 extracellular domain and membrane-bound cellular CD39.[64] We will investigate the effect of C_{39}Mab-1 on the enzymatic activity of mCD39 in future studies.

Recently, Zhang *et al*.[65] demonstrated the application of an anti-mCD39 mAb for tumor therapy by the depletion of immunosuppressive cells through enhanced Fcγ receptor–mediated antibody-dependent cellular cytotoxicity (ADCC). They found that mCD39 expression on tumor-infiltrating immune and vascular endothelial cells was markedly higher than that in normal tissues. They used a nonneutralizing anti-mCD39 mAb (clone 5F2, mouse IgG_1) and screened an isotype-switched hybridoma subline of the IgG_{2c} isotype which has more potent ADCC activities. To enhance the effector functions, the fucosyltransferase 8 gene was deleted in the 5F2 hybridomas using clustered regularly interspaced short palindromic repeats technology to produce the afucosylated antibody. They showed that the afucosylated anti-mCD39 IgG_{2c} exerted the potent antitumor effect against mouse melanoma and colorectal tumor models through the depletion of regulatory/exhausted T cells, tumor-associated

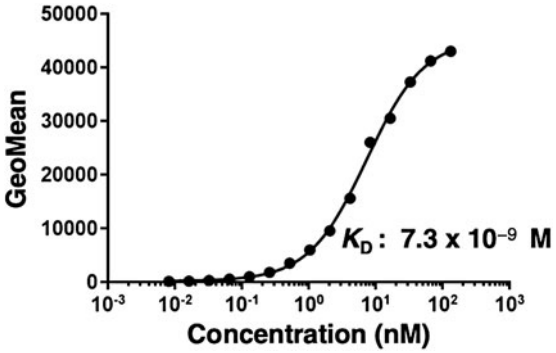

FIG. 3. The determination of the binding affinity of C_{39}Mab-1. CHO/mCD39 cells were suspended in 100 μL serially diluted C_{39}Mab-1 at the indicated concentrations. The cells were treated with Alexa Fluor 488-conjugated anti-rat IgG. The fluorescence data were subsequently collected using the SA3800 Cell Analyzer, following the calculation of the K_D by GraphPad PRISM 8. K_D, dissociation constant.

macrophages, and tumor vasculature with high mCD39 expression.

We previously produced recombinant antibodies, which were converted into mouse IgG_{2a} subclass from mouse IgG_1. Furthermore, we produced afucosylated IgG_{2a} mAbs using Fut8-deficient CHO-K1 cells to potentiate the ADCC activity. The afucosylated mAbs showed potent antitumor activity in mouse xenograft models.[66–73] Therefore, a class-switched and afucosylated version of C_{39}Mab-1 could be used to evaluate the antitumor activity *in vivo*.

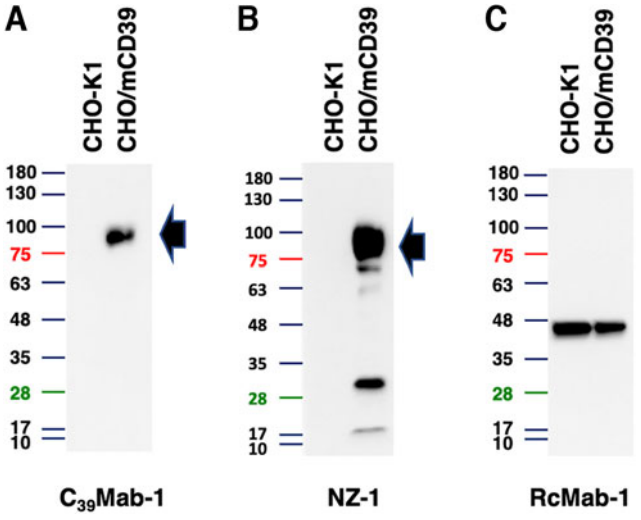

FIG. 4. Western blotting using C_{39}Mab-1. The cell lysates of CHO-K1 and CHO/mCD39 were electrophoresed and transferred onto PVDF membranes. The membranes were incubated with 10 μg/mL of C_{39}Mab-1 **(A)**, 1 μg/mL of NZ-1 (an anti-PA tag mAb) **(B)**, or 1 μg/mL of RcMab-1 (an anti-IDH1 mAb) **(C)**. The membranes were subsequently incubated with peroxidase-conjugated anti-rat immunoglobulins. The arrows indicate the predicted size of mCD39 (~100 kDa). PVDF, polyvinylidene fluoride.

Author Disclosure Statement

No competing financial interests exist.

Funding Information

This research was supported in part by Japan Agency for Medical Research and Development (AMED) under Grant Nos.: JP23ama121008 (to Y.K.), JP23am0401013 (to Y.K.), 23bm1123027h0001 (to Y.K.), and JP23ck0106730 (to Y.K.), and by the Japan Society for the Promotion of Science (JSPS) Grants-in-Aid for Scientific Research (KAKENHI) Grant Nos. 22K06995 (to H.S.), 21K07168 (to M.K.K.), and 22K07224 (to Y.K.).

References

1. Guo S, Han F, Zhu W. CD39—A bright target for cancer immunotherapy. Biomed Pharmacother 2022;151:113066; doi: 10.1016/j.biopha.2022.113066
2. Grygorczyk R, Boudreault F, Ponomarchuk O, et al. Lytic release of cellular ATP: Physiological relevance and therapeutic applications. Life (Basel) 2021;11; doi: 10.3390/life11070700
3. Moesta AK, Li XY, Smyth MJ. Targeting CD39 in cancer. Nat Rev Immunol 2020;20:739–755; doi: 10.1038/s41577-020-0376-4
4. Churov A, Zhulai G. Targeting adenosine and regulatory T cells in cancer immunotherapy. Hum Immunol 2021;82:270–278; doi: 10.1016/j.humimm.2020.12.005
5. Vijayan D, Young A, Teng MWL, et al. Targeting immunosuppressive adenosine in cancer. Nat Rev Cancer 2017;17:709–724; doi: 10.1038/nrc.2017.86
6. Sun C, Wang B, Hao S. Adenosine-A2A receptor pathway in cancer immunotherapy. Front Immunol 2022;13:837230; doi: 10.3389/fimmu.2022.837230
7. Ohta A, Sitkovsky M. Role of G-protein-coupled adenosine receptors in downregulation of inflammation and protection from tissue damage. Nature 2001;414:916–920; doi: 10.1038/414916a
8. Ohta A, Gorelik E, Prasad SJ, et al.: A2A adenosine receptor protects tumors from antitumor T cells. Proc Natl Acad Sci U S A 2006;103:13132–13137; doi: 10.1073/pnas.0605251103
9. Di Virgilio F, Sarti AC, Falzoni S, et al. Extracellular ATP and P2 purinergic signalling in the tumour microenvironment. Nat Rev Cancer 2018;18:601–618; doi: 10.1038/s41568-018-0037-0
10. Li XY, Moesta AK, Xiao C, et al. Targeting CD39 in cancer reveals an extracellular ATP- and inflammasome-driven tumor immunity. Cancer Discov 2019;9:1754–1773; doi: 10.1158/2159-8290.Cd-19-0541
11. Perrot I, Michaud HA, Giraudon-Paoli M, et al. Blocking antibodies targeting the cd39/cd73 immunosuppressive pathway unleash immune responses in combination cancer therapies. Cell Rep 2019;27:2411–2425.e2419; doi: 10.1016/j.celrep.2019.04.091
12. Yamada S, Kaneko MK, Sayama Y, et al. Development of novel mouse monoclonal antibodies against human CD19. Monoclon Antib Immunodiagn Immunother 2020;39:45–50; doi: 10.1089/mab.2020.0003
13. Furusawa Y, Kaneko MK, Kato Y. Establishment of C(20)Mab-11, a novel anti-CD20 monoclonal antibody, for the detection of B cells. Oncol Lett 2020;20:1961–1967; doi: 10.3892/ol.2020.11753

14. Furusawa Y, Kaneko MK, Kato Y. Establishment of an anti-CD20 monoclonal antibody (C(20)Mab-60) for immunohistochemical analyses. Monoclon Antib Immunodiagn Immunother 2020;39:112–116; doi: 10.1089/mab.2020.0015
15. Itai S, Fujii Y, Nakamura T, et al. Establishment of CMab-43, a sensitive and specific anti-CD133 monoclonal antibody, for immunohistochemistry Monoclon Antib Immunodiagn Immunother 2017;36:231–235; doi: 10.1089/mab.2017.0031
16. Li G, Suzuki H, Asano T, et al. Development of a novel anti-EpCAM monoclonal antibody for various applications. Antibodies (Basel) 2022;11; doi: 10.3390/antib11020041
17. Kaneko MK, Ohishi T, Takei J, et al. Anti-EpCAM monoclonal antibody exerts antitumor activity against oral squamous cell carcinomas. Oncol Rep 2020;44:2517–2526; doi: 10.3892/or.2020.7808
18. Itai S, Fujii Y, Kaneko MK, et al. H(2)Mab-77 is a sensitive and specific anti-HER2 monoclonal antibody against breast cancer. Monoclon Antib Immunodiagn Immunother 2017;36:143–148; doi: 10.1089/mab.2017.0026
19. Asano T, Ohishi T, Takei J, et al. Anti-HER3 monoclonal antibody exerts antitumor activity in a mouse model of colorectal adenocarcinoma. Oncol Rep 2021;46; doi: 10.3892/or.2021.8124
20. Asano T, Nanamiya R, Tanaka T, et al. Development of antihuman killer cell lectin-like receptor subfamily G member 1 monoclonal antibodies for flow cytometry. Monoclon Antib Immunodiagn Immunother 2021;40:76–80; doi: 10.1089/mab.2021.0008
21. Takei J, Asano T, Nanamiya R, et al. Development of anti-human T cell immunoreceptor with Ig and ITIM domains (TIGIT) monoclonal antibodies for flow cytometry. Monoclon Antib Immunodiagn Immunother 2021;40:71–75; doi: 10.1089/mab.2021.0006
22. Sayama Y, Kaneko MK, Takei J, et al. Establishment of a novel anti-TROP2 monoclonal antibody TrMab-29 for immunohistochemical analysis. Biochem Biophys Rep 2021;25:100902; doi: 10.1016/j.bbrep.2020.100902
23. Tanaka T, Ohishi T, Asano T, et al. An anti-TROP2 monoclonal antibody TrMab-6 exerts antitumor activity in breast cancer mouse xenograft models. Oncol Rep 2021;46; doi: 10.3892/or.2021.8083
24. Yamada S, Itai S, Nakamura T, et al. Monoclonal antibody L(1)Mab-13 detected human PD-L1 in lung cancers. Monoclon Antib Immunodiagn Immunother 2018;37:110–115; doi: 10.1089/mab.2018.0004
25. Yamada S, Itai S, Nakamura T, et al. PMab-52: Specific and sensitive monoclonal antibody against cat podoplanin for immunohistochemistry. Monoclon Antib Immunodiagn Immunother 2017;36:224–230; doi: 10.1089/mab.2017.0027
26. Furusawa Y, Kaneko MK, Nakamura T, et al. Establishment of a monoclonal antibody PMab-231 for tiger podoplanin. Monoclon Antib Immunodiagn Immunother 2019;38:89–95; doi: 10.1089/mab.2019.0003
27. Furusawa Y, Takei J, Sayama Y, et al. Development of an anti-bear podoplanin monoclonal antibody PMab-247 for immunohistochemical analysis. Biochem Biophys Rep 2019;18:100644; doi: 10.1016/j.bbrep.2019.100644
28. Furusawa Y, Yamada S, Itai S, et al. Establishment of a monoclonal antibody PMab-233 for immunohistochemical analysis against Tasmanian devil podoplanin. Biochem Biophys Rep 2019;18:100631; doi: 10.1016/j.bbrep.2019.100631
29. Goto N, Suzuki H, Tanaka T, et al. Development of a monoclonal antibody PMab-292 against ferret podoplanin. Monoclon Antib Immunodiagn Immunother 2022;41(2):101–109.
30. Furusawa Y, Yamada S, Itai S, et al. Establishment of monoclonal antibody PMab-202 against horse podoplanin. Monoclon Antib Immunodiagn Immunother 2018;37:233–237; doi: 10.1089/mab.2018.0030
31. Kato Y, Yamada S, Furusawa Y, et al. PMab-213: A monoclonal antibody for immunohistochemical analysis against pig podoplanin. Monoclon Antib Immunodiagn Immunother 2019;38:18–24.
32. Furusawa Y, Yamada S, Nakamura T, et al. PMab-235: A monoclonal antibody for immunohistochemical analysis against goat podoplanin. Heliyon 2019;5:e02063; doi: 10.1016/j.heliyon.2019.e02063
33. Kato Y, Furusawa Y, Yamada S, et al. Establishment of a monoclonal antibody PMab-225 against alpaca podoplanin for immunohistochemical analyses. Biochem Biophys Rep 2019;18:100633; doi: 10.1016/j.bbrep.2019.100633
34. Kato Y, Furusawa Y, Itai S, et al. Establishment of an anticetacean podoplanin monoclonal antibody PMab-237 for immunohistochemical analysis. Monoclon Antib Immunodiagn Immunother 2019;38:108–113.
35. Kato Y, Furusawa Y, Sano M, et al. Development of an anti-sheep podoplanin monoclonal antibody PMab-256 for immunohistochemical analysis of lymphatic endothelial cells. Monoclon Antib Immunodiagn Immunother 2020;39:82–90; doi: 10.1089/mab.2020.0005
36. Tanaka T, Asano T, Sano M, et al. Development of monoclonal antibody PMab-269 against California sea lion podoplanin. Monoclon Antib Immunodiagn Immunother 2021;40:124–133; doi: 10.1089/mab.2021.0011
37. Ejima R, Suzuki H, Tanaka T, et al. Development of a novel anti-CD44 variant 6 monoclonal antibody C(44)Mab-9 for multiple applications against colorectal carcinomas. Int J Mol Sci 2023;24; doi: 10.3390/ijms24044007
38. Yamada S, Itai S, Nakamura T, et al. Detection of high CD44 expression in oral cancers using the novel monoclonal antibody, C(44)Mab-5. Biochem Biophys Rep 2018;14:64–68; doi: 10.1016/j.bbrep.2018.03.007
39. Asano T, Nanamiya R, Takei J, et al. Development of anti-mouse CC chemokine receptor 3 monoclonal antibodies for flow cytometry. Monoclon Antib Immunodiagn Immunother 2021;40:107–112; doi: 10.1089/mab.2021.0009
40. Tanaka T, Nanamiya R, Takei J, et al. Development of anti-mouse CC chemokine receptor 8 monoclonal antibodies for flow cytometry. Monoclon Antib Immunodiagn Immunother 2021;40:65–70; doi: 10.1089/mab.2021.0005
41. Nanamiya R, Takei J, Asano T, et al. Development of anti-human CC chemokine receptor 9 monoclonal antibodies for flow cytometry. Monoclon Antib Immunodiagn Immunother 2021;40:101–106; doi: 10.1089/mab.2021.0007
42. Tamura R, Oi R, Akashi S, et al. Application of the NZ-1 Fab as a crystallization chaperone for PA tag-inserted target proteins. Protein Sci 2019;28:823–836; doi: 10.1002/pro.3580
43. Fujii Y, Matsunaga Y, Arimori T, et al. Tailored placement of a turn-forming PA tag into the structured domain of a protein to probe its conformational state. J Cell Sci 2016;129:1512–1522; doi: 10.1242/jcs.176685

44. Fujii Y, Kaneko M, Neyazaki M, et al. PA tag: A versatile protein tagging system using a super high affinity antibody against a dodecapeptide derived from human podoplanin. Protein Expr Purif 2014;95:240–247; doi: 10.1016/j.pep.2014.01.009
45. Miura K, Yoshida H, Nosaki S, et al. RAP tag and PMab-2 antibody: A tagging system for detecting and purifying proteins in plant cells. Front Plant Sci 2020;11:510444; doi: 10.3389/fpls.2020.510444
46. Fujii Y, Kaneko MK, Ogasawara S, et al. Development of RAP tag, a novel tagging system for protein detection and purification. Monoclon Antib Immunodiagn Immunother 2017;36:68–71; doi: 10.1089/mab.2016.0052
47. Fujii Y, Kaneko MK, Kato Y. MAP tag: A novel tagging system for protein purification and detection. Monoclon Antib Immunodiagn Immunother 2016;35:293–299; doi: 10.1089/mab.2016.0039
48. Wakasa A, Kaneko MK, Kato Y, et al. Site-specific epitope insertion into recombinant proteins using the MAP tag system. J Biochem. 2020;168:375–384;10.1093/jb/mvaa054
49. Kato Y, Kaneko MK, Kuno A, et al. Inhibition of tumor cell-induced platelet aggregation using a novel anti-podoplanin antibody reacting with its platelet-aggregation-stimulating domain. Biochem Biophys Res Commun 2006;349:1301–1307; doi: 10.1016/j.bbrc.2006.08.171
50. Chalise L, Kato A, Ohno M, et al. Efficacy of cancer-specific anti-podoplanin CAR-T cells and oncolytic herpes virus G47Delta combination therapy against glioblastoma. Mol Ther Oncolytics 2022;26:265–274; doi: 10.1016/j.omto.2022.07.006
51. Ishikawa A, Waseda M, Ishii T, et al. Improved anti-solid tumor response by humanized anti-podoplanin chimeric antigen receptor transduced human cytotoxic T cells in an animal model. Genes Cells 2022;27:549–558; doi: 10.1111/gtc.12972
52. Tamura-Sakaguchi R, Aruga R, Hirose M, et al. Moving toward generalizable NZ-1 labeling for 3D structure determination with optimized epitope-tag insertion. Acta Crystallogr D Struct Biol 2021;77:645–662; doi: 10.1107/S2059798321002527
53. Kaneko MK, Ohishi T, Nakamura T, et al. Development of core-fucose-deficient humanized and chimeric anti-human podoplanin antibodies. Monoclon Antib Immunodiagn Immunother 2020;39:167–174; doi: 10.1089/mab.2020.0019
54. Abe S, Kaneko MK, Tsuchihashi Y, et al. Antitumor effect of novel anti-podoplanin antibody NZ-12 against malignant pleural mesothelioma in an orthotopic xenograft model. Cancer Sci 2016;107:1198–1205; doi: 10.1111/cas.12985
55. Kaneko MK, Abe S, Ogasawara S, et al. Chimeric anti-human podoplanin antibody NZ-12 of lambda light chain exerts higher antibody-dependent cellular cytotoxicity and complement-dependent cytotoxicity compared with NZ-8 of kappa light chain. Monoclon Antib Immunodiagn Immunother 2017;36:25–29; doi: 10.1089/mab.2016.0047
56. Ito A, Ohta M, Kato Y, et al. A real-time near-infrared fluorescence imaging method for the detection of oral cancers in mice using an indocyanine green-labeled podoplanin antibody. Technol Cancer Res Treat 2018;17:1533033818767936; doi: 10.1177/1533033818767936
57. Shiina S, Ohno M, Ohka F, et al. CAR T cells targeting podoplanin reduce orthotopic glioblastomas in mouse brains. Cancer Immunol Res 2016;4:259–268; doi: 10.1158/2326-6066.CIR-15-0060
58. Kuwata T, Yoneda K, Mori M, et al. Detection of circulating tumor cells (CTCs) in malignant pleural mesothelioma (MPM) with the ''Universal'' CTC-chip and an anti-podoplanin antibody NZ-1.2. Cells 2020;9; doi: 10.3390/cells9040888
59. Nishinaga Y, Sato K, Yasui H, et al. Targeted phototherapy for malignant pleural mesothelioma: Near-infrared photoimmunotherapy targeting podoplanin. Cells 2020;9; doi: 10.3390/cells9041019
60. Kato Y, Kaneko MK, Kunita A, et al. Molecular analysis of the pathophysiological binding of the platelet aggregation-inducing factor podoplanin to the C-type lectin-like receptor CLEC-2. Cancer Sci 2008;99:54–61; doi: 10.1111/j.1349-7006.2007.00634.x
61. Kato Y, Vaidyanathan G, Kaneko MK, et al. Evaluation of anti-podoplanin rat monoclonal antibody NZ-1 for targeting malignant gliomas. Nucl Med Biol 2010;37:785–794; doi: 10.1016/j.nucmedbio.2010.03.010
62. Kato Y. Specific monoclonal antibodies against IDH1/2 mutations as diagnostic tools for gliomas. Brain Tumor Pathol 2015;32:3–11; doi: 10.1007/s10014-014-0202-4
63. Ikota H, Nobusawa S, Arai H, et al. Evaluation of IDH1 status in diffusely infiltrating gliomas by immunohistochemistry using anti-mutant and wild type IDH1 antibodies. Brain Tumor Pathol 2015;32:237–244; doi: 10.1007/s10014-01 5-0222-8
64. Spatola BN, Lerner AG, Wong C, et al. Fully human anti-CD39 antibody potently inhibits ATPase activity in cancer cells via uncompetitive allosteric mechanism. MAbs 2020;12:1838036; doi: 10.1080/19420862.2020.1838036
65. Zhang H, Feng L, de Andrade Mello P, et al.: Glycoengineered anti-CD39 promotes anticancer responses by depleting suppressive cells and inhibiting angiogenesis in tumor models. J Clin Invest 2022;132; doi: 10.1172/jci157431
66. Li G, Suzuki H, Ohishi T, et al. Antitumor activities of a defucosylated anti-EpCAM monoclonal antibody in colorectal carcinoma xenograft models. Int J Mol Med 2023;51; doi: 10.3892/ijmm.2023.5221
67. Nanamiya R, Takei J, Ohishi T, et al. Defucosylated anti-epidermal growth factor receptor monoclonal antibody (134-mG(2a)-f) exerts antitumor activities in mouse xenograft models of canine osteosarcoma. Monoclon Antib Immunodiagn Immunother 2022;41:1–7; doi: 10.1089/mab.2021.0036
68. Kawabata H, Suzuki H, Ohishi T, et al. A defucosylated mouse anti-CD10 monoclonal antibody (31-mG(2a)-f) exerts antitumor activity in a mouse xenograft model of CD10-overexpressed tumors. Monoclon Antib Immunodiagn Immunother 2022;41:59–66;10.1089/mab.2021.0048
69. Kawabata H, Ohishi T, Suzuki H, et al. A defucosylated mouse anti-CD10 monoclonal antibody (31-mG(2a)-f) exerts antitumor activity in a mouse xenograft model of renal cell cancers. Monoclon Antib Immunodiagn Immunother 2022;41(6):320–327; doi: 10.1089/mab.2021.0049
70. Asano T, Tanaka T, Suzuki H, et al. A defucosylated anti-EpCAM monoclonal antibody (EpMab-37-mG(2a)-f) exerts antitumor activity in xenograft model. Antibodies (Basel) 2022;11(4):74; doi: 10.3390/antib11040074
71. Tateyama N, Nanamiya R, Ohishi T, et al. Defucosylated anti-epidermal growth factor receptor monoclonal antibody

134-mG(2a)-f exerts antitumor activities in mouse xenograft models of dog epidermal growth factor receptor-overexpressed cells. Monoclon Antib Immunodiagn Immunother 2021;40: 177–183; doi: 10.1089/mab.2021.0022

72. Takei J, Ohishi T, Kaneko MK, et al. A defucosylated anti-PD-L1 monoclonal antibody 13-mG(2a)-f exerts antitumor effects in mouse xenograft models of oral squamous cell carcinoma. Biochem Biophys Rep 2020;24:100801; doi: 10 .1016/j.bbrep.2020.100801
73. Takei J, Kaneko MK, Ohishi T, et al. A defucosylated antiCD44 monoclonal antibody 5mG2af exerts antitumor effects in mouse xenograft models of oral squamous cell carcinoma. Oncol Rep 2020;44:1949–1960; doi: 10.3892/ or.2020.7735

Address correspondence to:
Yukinari Kato
Department of Antibody Drug Development
Tohoku University Graduate School of Medicine
2-1, Seiryo-machi
Aoba-ku
Sendai
Miyagi 980-8575
Japan

E-mail: yukinari.kato.e6@tohoku.ac.jp

Received: September 1, 2023
Accepted: September 15, 2023